Structural and functional analysis of critical amino acids in TMVI of the NHE1 isoform of the Na$^+$/H$^+$ exchanger

Jennifer Tzeng, Brian L. Lee, Brian D. Sykes, Larry Fliegel *

Department of Biochemistry, University of Alberta, Edmonton, Alberta, Canada T6G 2H7

ARTICLE INFO

ABSTRACT

The mammalian Na$^+$/H$^+$ exchanger isoform 1 (NHE1) resides on the plasma membrane and exchanges one intracellular H$^+$ for one extracellular Na$^+$. It maintains intracellular pH and regulates cell volume, and cell functions including growth and cell differentiation. Previous structural and functional studies on TMVI revealed several amino acids that are potentially pore lining. We examined these and other critical residues by site-directed mutagenesis substituting Asn227 → Ala, Asp, Arg; Ile233 → Ala; Leu243 → Ala; Glu247 → Asp, Gln; Glu248 → Asp, Gln. Mutant NHE1 proteins were characterized in AP-1 cells, which do not express endogenous NHE1. All the TMVI critical amino acids were highly sensitive to substitution and changes often lead to a dysfunctional protein. Mutations of Asn227 → Ala, Asp, Arg; Ile233 → Ala; Leu243 → Ala; Glu247 → Asp; Glu248 → Gln yielded significant reduction in NHE1 activity. Mutants of Asn227 demonstrated defects in protein expression, targeting and activity. Substituting Asn227 → Arg and Ile233 → Ala decreased the surface localization and expression of NHE1 respectively. The pore lining amino acids Ile233 and Leu243 were both essential for activity. Glu247 was not essential, but the size of the residue at this location was important while the charge on residue Glu248 was more critical to NHE1 function. Limited trypsin digestion on Leu243 → Ala and Glu248 → Gln revealed that they had increased susceptibility to proteolytic attack, indicating an alteration in protein conformation. Modeling of TMVI with TMXI suggests that these TM segments form part of the critical fold of NHE1 with Ile233 and Leu465 of TMXI forming a critical part of the extracellular facing ion conductance pathway.

© 2011 Elsevier B.V. All rights reserved.

1. Introduction

The Na$^+$/H$^+$ exchangers (NHE) are membrane proteins present in all known eukaryotic and prokaryotic cells. In mammalian cells, their primary role is to regulate intracellular pH (pH$_i$), maintaining physiological pH despite acid load from cellular metabolism. Ten mammalian Na$^+$/H$^+$ exchanger isoforms have been discovered. The first isoform, NHE1, was cloned in 1989 [1] by Pouyssegur's group and since that time numerous functional studies have led to the understanding of its importance in cell regulation and have identified other NHE isoforms [2,3]. NHE1 is ubiquitously expressed on the plasma membrane, while NHE2–NHE10 are distributed among specific cell types, and have different kinetic characteristics, different membrane localization and are regulated differently [4,5]. NHE1 carries out the pH$_i$ sensitive exchange of one intracellular H$^+$ for an extracellular Na$^+$. This is important because variations in pH$_i$ are capable of disrupting normal protein folding, chemical reactions and ion gradients [6]. In addition to pH$_i$ and volume regulation, NHE1 is also essential for cell growth, differentiation, and migration [7–10]. Increased NHE1 levels and activity also have pathological roles in cancer development, cardiac ischemia reperfusion injury, and cardiac hypertrophy [11–15]. Therefore, inhibitors of NHE1 have been investigated for their efficacy of treating cancer and heart disease [15–18].

NHE1 is composed of two domains with 815 amino acids with an apparent molecular weight of 110 kDa in the N-linked and O-linked glycosylated form [4,13,19]. The N-terminal domain consists of approximately 500 residues, which form the 12 transmembrane segments that span the plasma membrane and arrange into a structure for cation translocation. The latter 315 residues of NHE1 form the cytoplasmic regulatory tail that contains phosphorylation sites, and binding sites for PIP$_2$, ERM (ezrin/radixin/moesin), tescalcin, 14-3-3, carbonic anhydrase, calmodulin, calcineurin homologous protein type 1 and calcineurin homologous protein type 2 [2,3,9,10,20].

Attempts are underway to determine the high resolution crystal structure of NHE1. However, several avenues of study have used

homology model analysis, mutational analysis, NMR spectroscopy and electron microscopy to reveal significant insights into the secondary and tertiary structure of NHE1 [21–24]. As part of a series of studies analyzing the structure and function of transmembrane regions of NHE1 [21,25,26] we recently analyzed the peptide structure of TMVI (N227–I249) of NHE1 in DPC micelles, and analyzed the functional contribution of amino acids of that segment by using the cysteine scanning accessibility method [27]. Many amino acid residues of TMVI (transmembrane segment VI) were sensitive to mutation to Cys and reaction with external sulfhydryls indicating that TMVI was a critical pore lining segment. Interestingly, TMVI had a structure consisting of a helix, extended region, followed by a helix. This was similar in structure to the critical TMIV of the *Escherichia coli* Na$^+$/H$^+$ exchanger NhaA and we proposed that it serves a similar critical role in NHE1 activity. In this study we further characterized this key transmembrane segment. Of the residues in TMVI that maintained sufficient NHE1 activity when substituted to Cys, the key pore lining amino acids of TMVI were Asn227, Ile233 and Leu243. Several other residues had partially depressed activity when substituted to cysteine including, Glu247 and Glu248. Moreover, the Glu248→Cys mutant was partially inhibited by MTSET treatment [27]. Here we further characterized the functional importance of critical amino acids in TMVI. Applying site-directed mutagenesis methods, Asn227, Ile233, Leu243, Glu247, and Glu248 of TMVI were substituted into Asn227→Ala, Asp, Arg; Ile233→Ala; Leu243→Ala; Glu247→Asp, Gln; Glu248→Asp, Gln. These mutant NHE1 proteins were assessed for their protein expression, activity, and surface localization. Limited digestion with trypsin was used to examine protein conformational changes caused by mutations. Additional structural modeling was performed based on previous NMR studies of TMVI and XI to investigate their assembly in the cation translocation pore. Our results demonstrate that TMVI forms a critical part of the cation access pathway along with TMXI. Asn227 and Ile233 form part of the extracellular facing pore while Leu243, Glu247 and Glu248 form critical parts of the intracellular fold of the coordination pathway.

2. Materials and methods

2.1. Materials

PWO DNA polymerase was purchased from Roche Applied Science (Roche Molecular Biochemicals, Mannheim, Germany). Restriction enzymes were obtained from New England Biolabs, Inc. (Mississauga ON, Canada). Lipofectamine™ 2000 reagent was purchased from Invitrogen Life Technologies (Carlsbad CA, USA). 2′,7′-bis (2-carboxyethyl)-5(6) carboxyfluorescein-acetoxymethyl ester was purchased from Molecular probes, Inc. (Eugene OR, USA). Sulpho-NHS-SS-Biotin was from Pierce Chemical Company (Rockford IL, USA). Immobilized streptavidin resin, nigericin and trypsin (phenylalanyl chloromethyl ketone-trypsin) were from Sigma-Aldrich (St Louis MO, USA). Geneticin G418 antibiotics were purchased from American Bioanalytical (Natick MA, USA). Cell culture MEM alpha modification medium was from Thermo Scientific Hyclone (Logan UT, USA).

2.2. Site-directed mutagenesis

Silent mutation restriction enzyme sites were introduced for selection as described earlier [23]. We used the plasmid pYN4+ as a template, which encoded for the entire human NHE1 and a hemagglutinin (HA) tag at the C-terminal end [23]. The HA-tagged NHE1 functions normally as the wild type NHE1 [21]. The oligomers for site directed mutagenesis are indicated in Table 1. Site-directed mutagenesis was performed using PWO DNA polymerase from the Stratagene (La Jolla, CA, USA) QuikChange™ site directed mutagenesis

Table 1
Oligonucleotides used for site-directed mutagenesis of TMVI. Nucleotides mutated are indicated in lower case, and restriction sites introduced are indicated in bold.

A		
Mutation	Oligonucleotide sequence	Restriction site
N227A	5′-CAACAACATCGGCCT**tCTaGAC**gcCCTGCTCTTCGGCAGC-3′	*Xba I*
N227D	5′-CAACAACATCGGCCT**tCTaGAC**gACCTGCTCTTCGGCAGC-3′	*Xba I*
N227R	5′-CAACAACATCGGCCT**tCTaGAC**cgCCTGCTCTTCGGCAGC-3′	*Xba I*
I233A	5′-CTGCTCTTC**GGatcC**gcCATCTCGGCCGTGGAC-3′	*Bam HI*
L243A	5′-GACCCCGTGGCGGTTg**ccGCg**GTCTTTGAGGAAATT-3′	*Sac II*
E247D	5′-GTTCTGGCTGTCTTTGAcGA**gAtT**CAC**ATC**AATGAG-3′	*Bsa BI*
E247Q	5′-GTTCTGGCTGTCTTTcAGGA**gAtT**CAC**ATC**AATGAG-3′	*Bsa BI*
E248D	5′-TCTGGCTGTC**TTcGAa**GAcATTCACATCAATGAG-3′	*Bst BI*
E248Q	5′-TCTGGCTGTC**TTcGAacAA**ATTCACATCAATGAG-3′	*Bst BI*

kit. DNA sequencing was performed at the University of Alberta, Department of Biochemistry DNA Core Services Lab.

2.3. Cell culture and transfections

Mutant plasmids were transfected in the AP1 cell line, which does not express endogenous active NHE1. AP-1 is a mutant cell line derived from Chinese hamster ovarian cells (CHO) by proton suicide technique [1]. Stably transfected cells were established using LIPOFECTAMINE™ 2000 Reagent (Invitrogen Life Technologies, Carlsbad, CA, USA) as described earlier [21]. pYN4+ plasmid encoded a neomycin resistance gene, which allowed the selection of transfected cells using geneticin (G418) antibiotics. Stable cell lines for experiments were regularly re-established from frozen stocks at passage numbers between 5 and 11.

2.4. SDS-PAGE and immunoblotting

Cells were cultured in 60 or 35 mm dishes until 80–90% confluent, and then were harvested as described earlier [26]. Growth medium was removed by aspiration and cell monolayers were washed with 4 °C phosphate-buffered saline. Plates were kept on ice to reduce protein degradation. RIPA Lysis buffer (1% NP-40, 0.25% sodium deoxycholate, 0.1% Triton X-100, 5 mM EGTA, 0.1 mM phenylmethyl-sulfonyl fluoride, 0.1 mM benzamidine, protease inhibitor cocktail) was added to AP-1 cells for 1–3 min. Cell debris were removed by centrifugation at 14,000 rpm for 5 min at 4 °C. Supernatants were kept in clean eppendorf tubes and they were either frozen for −80 °C storage or prepared for subsequent trypsin treatment and SDS-PAGE. Cell lysates containing NHE1 were resolved on 10% SDS/polyacrylamide gels. Proteins were transferred onto nitrocellulose membrane (BioRad) and detected using anti-HA monoclonal antibody. The secondary antibody was peroxidase-conjugated goat anti-mouse antibody. NHE1 was visualized by enhanced chemiluminescence, and X-ray films (Fuji medical X-ray film) were processed by Kodak X-OMAT 2000 M35 processor. ImageJ 1.35 software (National Institutes of Health, Bethesda, MD, USA) was used to quantify band intensities.

2.5. Cell surface expression

Targeting of NHE1 to the cell surface was examined essentially as described earlier [21,26]. Cells were grown to 50–70% confluence in 60 mm dishes. The plates were placed on ice, washed once with 4 °C PBS followed by a second wash with 4 °C borate buffer pH9 (154 mM NaCl, 7.2 mM KCl, 1.8 mM CaCl$_2$, 10 mM boric acid). 3 ml of freshly made sulpho-NHS-SS-Biotin (Pierce Chemical Company, Rockford, IL, USA) at a concentration of 0.5 mg/ml in borate buffer was added to each plate and cells were incubated for 30 min at 4 °C. Cells were then washed 3 times with cold quenching buffer pH 8.3 (192 mM glycine,

25 mM Tris) on ice. Solubilization of cells was achieved by addition of 500 μl IP lysis buffer pH7.5 (1% (w/v) deoxycholic acid, 1% (w/v) Triton X-100, 0.1% (w/v) SDS, 150 mM NaCl, 1 mM EDTA, 10 mM Tris/Cl, 0.1 mM phenylmethylsulfonyl fluoride, 0.1 mM benzamidine, and lab-made protease inhibitor cocktail). Cell debris was removed by centrifugation at 16,000 g at 4 °C for 20 min. Supernatants were transferred into two equal 200 μl fractions in eppendorf tubes, to a "Total" fraction and an "Unbound" fraction. We have found [21,26] that bound labeled NHE1 does not reliably elute from streptavidin resin so we examined total and unbound fractions. In the unbound fraction, 50 μl of immobilized strepavidin resin was added to bind the biotin labeled proteins. Unbound fractions were then incubated at 4 °C overnight with gentle rocking. Supernatans were collected the following day by centrifugation at 16,000 g for 2 min. 25 μl of the total fraction and 28 μl of unbound fraction were loaded on 10% acrylamide gels for SDS-PAGE. NHE1 was detected by western blotting, and quantified using Image J software.

2.6. Na$^+$/H$^+$ exchange activity

NHE1 activity was determined essentially as described earlier [7,21]. All activity assays were performed on independently made clones of each TMVI cysteine mutant stable cell lines using a PTI Deltascan spectrofluorometer. Experiments were performed at 37 °C and all solutions and relevant equipment were pre-warmed to 37 °C. WT, cNHE1, and TMVI mutants were cultivated on coverslips (Thomas® Red Label® Micro Cover Glasses) in 35 mm dishes until more than 80% confluent. Cells were then incubated in 400 μl serum free α-MEM medium containing 1.875 μg/ml 2′,7′-bis(2-carboxyethyl)-5(6) carboxyfluorescein-acetoxymethyl ester (BCECF-AM; Molecular Probes Inc., Eugene, OR, USA) for 20 min to allow BCECF-AM to penetrate into the cell. The coverslip was attached to a coverslip holder, placed in a cuvette filled with 2.5 ml normal buffer pH7.3 (135 mM NaCl, 5 mM KCl, 1.8 mM CaCl$_2$, 1 mM MgSO$_4$, 5.5 mM glucose, 10 mM hepes) and left in the fluorometer for 3 min. 50 μl of 2.5 M ammonium chloride was added and the cells were incubated for another 3 min. After this time the solution was changed to 2.5 ml sodium free buffer pH7.3 (135 mM N-methyl glucamine, 5 mM KCl, 1.8 mM CaCl$_2$, 1 mM MgSO$_4$, 5.5 mM glucose, 10 mM hepes) for 30 s. This step allowed the removal of the external ammonium chloride and induced transient intracellular acidification. Cells were then returned to normal sodium containing buffer, allowing pH recovery via the activity of NHE1. Each measurement of NHE1 activity was followed by a 3 point pH calibration to calibrate the amount of fluorescence to pH$_i$. pH calibration buffers at a pH of 6, 7, and 8 were used (5 mM N-Methyl Glucamine, 135 mM KCl, 1.8 mM CaCl$_2$, 1 mM MgSO$_4$, 5.5 mM glucose, 10 mM HEPES, pH adjusted with KOH and HCl). The first 20 s of recovery was used to calculate the NHE1 activity.

2.7. Limited trypsin digestion

Limited trypsin digestion of the NHE1 protein was used to determine changes in conformation of the protein as described earlier [28]. Cell lysates were prepared as described above using RIPA lysis buffer, with the exception that proteinase inhibitors phenylmethylsulfonyl fluoride, benzamidine and protease cocktail were not added. Trypsin (phenylalanyl chloromethyl ketone-trypsin, Sigma, St., Louis, MO) was prepared and dissolved in TE buffer. Equal amounts of proteins (100 μg) from cell lysates were treated with trypsin at different trypsin:protein ratios (1:1500, 1:2000, 1:2500, 1:3000) and incubated at 37 °C for 5 min. The reaction was terminated by addition of SDS-PAGE loading buffer followed by boiling at 100 °C for 5 min. Samples were resolved by SDS-PAGE and NHE1 detected by western blot analysis. Quantification of the band intensity was done using ImageJ 1.35 software (National Institutes of Health, Bethesda, MD, USA). To minimize variation we compared the level of fully glycosylated NHE1 protein in mutant proteins to that of the wild type protein treated simultaneously and run on the same gel.

2.8. Modeling of the predicted functional assembly of NHE1

Restraints defining the secondary structure of both TMVI and TMXI were obtained from the previously published NMR structures of synthetic peptides representing TMVI and TMXI in dodecylphosphocholine micelles [25,27]. Additional restraints defining the interaction between TMVI and TMXI were measured from the three-dimensional model of NHE1 by Landau et al. [22] which proposes that TMVI and TMXI are equivalent to the discontinuous helices TMIV and TMXI found in the crystal structure of NhaA [29]. All interhelical distances between protons less than 4 Å were used. These distances were converted to restraints with a range of 1.8–4 Å for the calculation of the model. Calculation of the final model structure used the distance and dihedral restraints from the NMR structure calculation of TMVI and TMXI combined with the interhelical distance restraints obtained from the model of Landau et al. [22]. An ensemble of 50 structures were calculated, from which the 25 lowest energy structures were used to calculate an average structure. Calculation of the model was performed using simulated annealing in xplor-nih 2.26 [30] through the python scripting interface.

2.9. Statistical analysis

Results are shown as mean ± SE and statistical significance was determined using a Mann–Whitney U test.

3. Results

3.1. Analysis of amino acids of TMVI critical for NHE1 activity

We have previously [27] demonstrated that TMVI of NHE1 is a pore lining segment with several specific amino acids of TMVI identified as pore lining residues and with other residues having depressed NHE1 activity when mutated to Cys. We therefore decided to further investigate the characteristics of the critical pore lining residues Asn227, Ile233, Leu243, and other residues (Glu247 and Glu248) important for activity. Nine mutations of various types were made to replace these residues in the background of wild type NHE1 protein. Hydrophilic Asn227 was mutated to an Ala with a small side chain group, also to a Gln with longer hydrophilic side chain, and to a positively charged Arg. Ile233 and Leu243 were mutated to Ala to remove the contribution of their long hydrophobic side chains. Glu247 and Glu248 were mutated into similar charged, but smaller Asp and to a polar Gln side chain that does not have a free carboxyl. All TMVI mutant plasmids were successfully transfected in AP-1 cells and the expressed NHE1 protein was detected by SDS-PAGE and subsequent western blotting against the HA tag. Initial experiments determined the expression levels of each TMVI mutant protein (Fig. 1). NHE1 has two forms: the mature NHE1 is glycosylated and has a higher molecular weight at around 105–110 kDa, whereas the immature form of NHE1 is partially or non-glycosylated with a molecular weight around 85–95 kDa. Both forms were present in our stably expressing cells. Some of the mutants expressed reduced amounts of NHE1 protein. L243A and E248Q had expression reduced to ~90% and ~75% of control NHE1 respectively. I233A displayed the lowest expression of NHE1 expression at only 44% of wild type. Mutation of Asn227 → Arg reduced expression of the mature form of NHE1 drastically and the immature protein made up the majority of NHE1 expressed. We have previously found that mutation of some other residues of NHE1 had the same effect including the mutations I145C, Y4554C and G459C [25].

The surface localization of TMVI mutants was investigated. Membrane proteins are usually synthesized in the endoplasmic
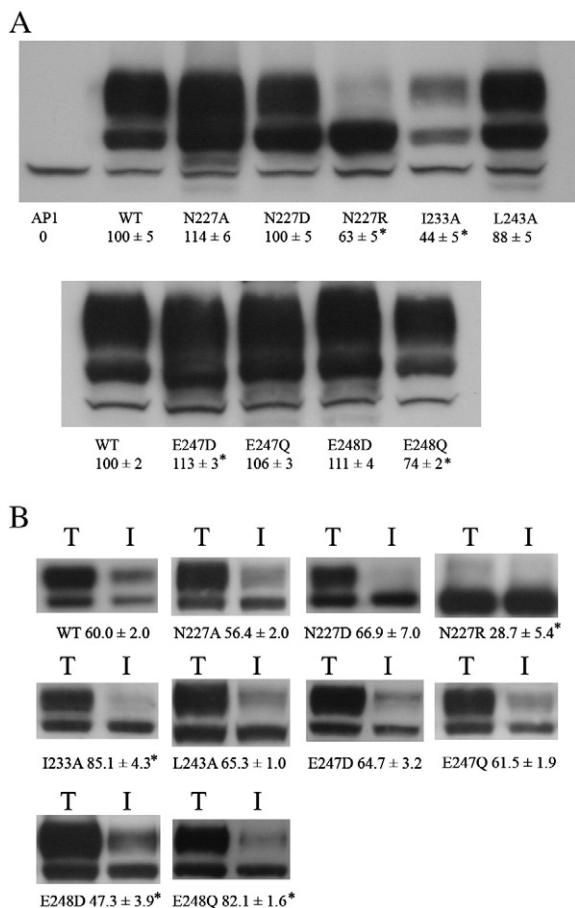
A

AP1	WT	N227A	N227D	N227R	I233A	L243A
0	100 ± 5	114 ± 6	100 ± 5	63 ± 5*	44 ± 5*	88 ± 5

WT	E247D	E247Q	E248D	E248Q
100 ± 2	113 ± 3*	106 ± 3	111 ± 4	74 ± 2*

B

T	I	T	I	T	I	T	I
WT 60.0 ± 2.0		N227A 56.4 ± 2.0		N227D 66.9 ± 7.0		N227R 28.7 ± 5.4*	

T	I	T	I	T	I	T	I
I233A 85.1 ± 4.3*		L243A 65.3 ± 1.0		E247D 64.7 ± 3.2		E247Q 61.5 ± 1.9	

T	I	T	I
E248D 47.3 ± 3.9*		E248Q 82.1 ± 1.6*	

Fig. 1. Characterization of expression of NHE1 mutant proteins. A. NHE1 expression levels of mutants of critical residues in TMVI. Western blot analysis of whole cell extracts of WT NHE1, and TMVI mutants. Each lane contained 75 g of total protein. The specific mutations are indicated. AP1 indicates untransfected-control cell lysates. NHE1 expression levels were examined using anti-HA antibody. Numbers underneath the lanes indicate the mean value (± SE) of the sum of densitometric scans of both 110 kDa and 95 kDa bands relative to wild-type NHE1 for at least three experiments. * indicates mutants with significantly different expression than WT NHE1 at P < 0.05. B. Surface localization of NHE1 proteins with mutations in critical residues of TMVI. Sulfo-NHS-SS-biotin treated cells were lysed and their proteins were solubilized and subsequently treated as described in the "Materials and Methods". Equal samples of total lysates (T) and unbound (representing intracellular) lysates (U) were resolved on SDS-PAGE and probed with anti-HA antibody to identify NHE1 protein. The amount of surface localized fully glycosylated NHE1 was calculated from densitometric analysis by taking the (total protein) – (unbound protein) = (membrane surface localized protein). The percent of the total NHE1 protein localized to the plasma membrane is indicated. Results are mean ± SE, n = at least 6 experiments. * Indicates significantly reduced plasma membrane targeting in comparison to wild type (WT) NHE1 (P < 0.05).

reticulum, processed further in the golgi bodies, and targeted to membrane destinations. Previous studies have found that mutations in NHE1 may interrupt the synthesis and transport network, which causes intracellular retention of the mutant protein and is reflected in impaired restoration of acidified pH$_i$ [25,31,32]. Surface targeting experiments were carried out as described in the "Materials and methods". The total and unbound (intracellular) fractions of cell lysates were examined by SDS-PAGE and western blotting, and the amount of fully glycosylated and partially/non-glycosylated NHE1 were measured. The results are shown in Fig. 1B and Supplementary Table 1. Examination of the fully glycosylated NHE1 protein demonstrated that the amount of NHE1 targeted to the cell surface declined significantly for both N227R and E248D mutants (Fig. 1B). N227R targeted to the cell surface about half as well as the control. I233A and E248Q displayed ~20% higher localization of mature glycosylated NHE1 protein to the cell

surface. There was also a ~10% significant reduction in the glycosylated form of the E248D mutant on the plasma membrane. The mature fully glycosylated NHE1 protein generally targeted to the membrane surface, whereas the immature partially glycosylated NHE1 largely remained mainly intracellular (Supplementary Table 1). However significant amounts of partially- or unglycosylated NHE1 protein were also present on the cell surface similar to results we have observed earlier [27]. Examination of the individual plasma membrane targeting of the fully glycosylated and partially or de-glycosylated forms of the mutants showed that targeting was impaired in several other cases, this included in all Asn227 mutants and in L243A and E248D (Supplementary Table 1).

The cation transport activity of NHE1 TMVI mutant stable cell lines was examined by assessing their ability to recover from a transient intracellular acidification. The results are shown in Fig. 2. Fig. 2A illustrates an example of a time course of transient intracellular acidifications followed by recoveries. The graph in Fig. 2B indicates the uncorrected NHE1 activities in black bars and hatched bars are activities normalized with expression levels and levels of surface localization of the mature form of NHE1. Supplementary Table 1 illustrates the raw NHE1 activities prior to correction with protein expression levels and surface expression. Some mutant NHE1 proteins had nearly no signs of pH$_i$ recovery after intracellular acidification (N227R, I233A, and L243A). N227A exhibited ~75% of control activity. N227D and E248Q had less than 40% of control activity. Correcting the raw activities for protein expression and localization, did not revert activity back to wild type NHE1 levels indicating that the effect of the mutations on activity were due to effects on actual activity of the NHE1 proteins, and not due to aberrant targeting or expression levels.

Of the nine TMVI mutations four residues, I233A, L243A, E247D, and E248Q were chosen for further investigation to determine the nature of the defect in NHE1 activity. Limited trypsin digestions were carried out to determine if there were changes in protein conformation [28,33]. Cell lysates were treated with trypsin for 5 min and at different ratios of trypsin:protein (1:1500 to 1:3000 as indicated) to produce fragments of NHE1 protein. Control digestions of wild type NHE1 protein were always done simultaneously with the mutants to make experimental results more uniform. The results (Fig. 3A–E) showed that there was no significant difference between the digestion pattern of NHE1 control, E247D and I233A mutant proteins. E248Q displayed a higher sensitivity to trypsin than the wild type, and most of the immunoreactive NHE1 bands disappeared even at the lowest trypsin:protein ratio of 1:3000. Other mutants were slightly more susceptible to trypsin hydrolysis compared to WT NHE1. For L243A, most of the bands were digested in the L243A mutant at 1:2000 trypsin:protein ratio treatment. There was no appearance of additional bands due to trypsin digestion. Western blot analysis was done using the HA-tag at the C-terminal tail of NHE1.

3.2. Molecular modeling of TMVI and TMXI

NhaA, a bacterial homologue to the human Na$^+$/H$^+$ exchanger NHE1, contains two discontinuous helices, TMIV and TMXI [22]. These helices are thought to be central to the alternating-exchange mechanism in the transporter. In the model of NHE1 developed by Landau et al., [22] they suggested that TMVI and XI are functionally and structurally equivalent to TMIV and XI, respectively, of NhaA. We previously determined the structure of peptides of TMVI and TMXI using high-resolution solution-state NMR in dodecylphosphocholine micelles and found that TMXI of NHE1 is similar in structure to TMXI of NhaA [25], and that TMVI of NHE1 is similar in structure to TMIV of NhaA [27]. Both TMVI and TMXI contained two helical regions connected by a flexible, extended region, similar to the structure of the discontinuous helices of TMIV and XI NhaA [22], suggesting we could model our NMR structures into a similar conformation. To generate a model of the NMR structures of interacting TMVI and TMXI, experimental NMR restraints from the individual helices were
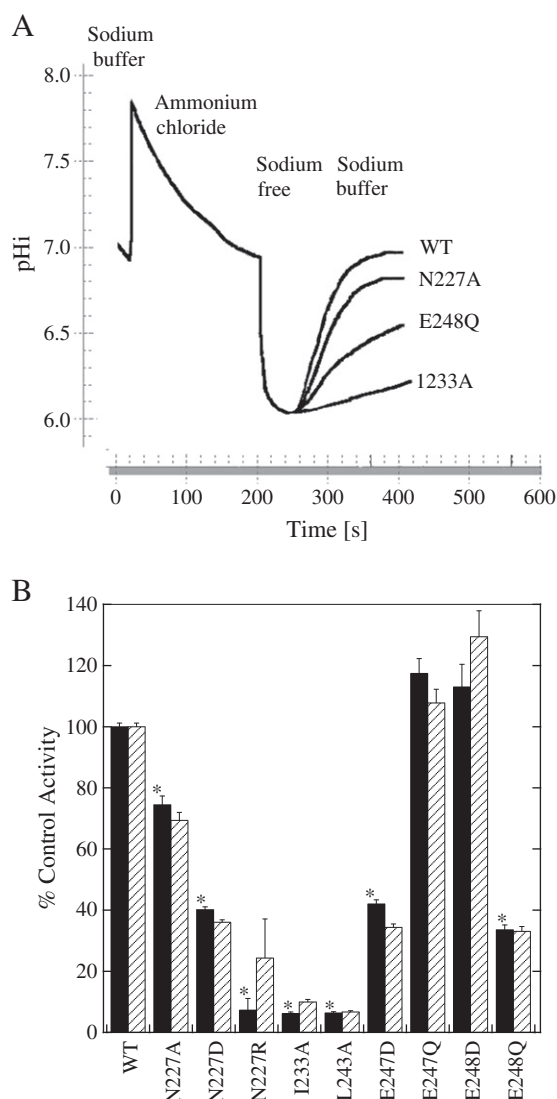
A

B

Fig. 2. Characterization of NHE1 activity of mutants of critical residues in TMVI. A. Example of activity traces of wild type and mutant NHE1 proteins. The activity of WT NHE1 protein is shown. For clarity, only the pHi recovery after acidosis is illustrated for the mutant proteins N227A, I233A, and E248Q. B. Summary of NHE activity of mutant NHE1 proteins. The activities of NHE1 WT control, and TMVI mutants were determined as described in "Materials and methods". The rate of recovery in WT NHE1 was set to 100% and mutants' recovery rates were expressed as a percent of WT. Results are mean ± S.E. (n = at least 6 determinations). Solid bars are NHE1 activities as measured, not corrected for the level of protein expressed or surface targeting. Hatched bars indicate NHE1 activity corrected for expression levels and surface targeting. * indicates uncorrected TMVI mutant activities that are significantly lower than that of WT NHE1 at P<0.05.

combined with restraints based on the Landau 3D model of NHE1. Restraints defining the structure of each of the TMs were defined by the previously published NMR distance and dihedral restraints [25,27]. Restraints for the interaction between the TMs were obtained from the Landau model [22], with inter-TM proton-proton distances less than 4 Å set as distance restraints with a range of 1.8–4 Å. These restraints were combined and used to generate 50 structures. An average structure calculated from the 25 lowest energy structures is shown in Fig. 4A.

The secondary structures of TMVI and TMXI in this model are the same as in the NMR structures. TMVI consists of two helical regions, at residues 229–236 and 239–250, separated by a short extended region at residues 237–238. Residues 223–228 are flexible in the model as in the NMR structure. TMXI has a similar structure, with two helical

regions at residues 447–454 and 460–471, with an extended region at residues 455–459. The orientation of the helices in TMVI is also approximately the same as the earlier published NMR structure [27], with the two helical regions at right angles to each other. TMXI, which had much variability in the orientation of its helices in the NMR structure [25], also adopts a right angled conformation, likely adopting to the conformation of TMVI.

TMVI and TMXI from the model of Landau et al. [22] are shown in Fig. 4B. The helical regions for TMXI in the Landau model are almost the same as the NMR model (residues 448–454 and 460–470). The N-terminal helix in TMVI is different. Residues 227–232 form a helix, while 233–236 form a distorted helix. This difference in structure results in many restraint violations in this region in the NMR model shown in Fig. 4A. In the C-terminal helix, residues 240–246 in the Landau model are helical, making this shorter than in the NMR based model. The lysine tags in the NMR based model are not present in the native protein structure or in the model of Landau et al. [22]. In Fig. 4B it can be seen that the axes of the C-terminal helices of TMVI and TMXI are parallel, while in Fig. 4A they are tilted away from vertical, towards the N-terminal helices of TMVI and TMXI. The interhelical restraints result in the orientation of side chains in the interface of the NMR model to be generally similar in the Landau model, while the orientation of side chains away from the interface tends towards the results obtained with NMR measurements.

We examined the relative position of the mutated amino acids of TMVI in two model structures of TMVI. The amino acids mutated in this study are indicated. In Fig. 4A, Asn227 which was essential for activity, is on the extracellular face of the membrane, possibly on the extracellular loop, and could be part of the mouth or funnel of the protein. Ile233 is in close association with TMXI, perhaps mediating inter-TM associations but also possibly lining a potential pore region. It is near to Leu465 which was a pore lining residue of TMXI [25,27]. The essential amino acid Leu243 is facing slightly away from region between the two TM segments but points along the same face as Leu465. Both Glu247 and Glu248 are in or near the cytosolic face of the protein. The charge on Glu248 was essential for activity and it is interesting that it faces away from the direction of the side chain of Leu243. Glu247 is on a similar side as Leu243 and Leu465.

Fig. 4B illustrates a model of TMVI and TMXI based upon the predictions of Landau et al. [22]. There are similarities and some differences from Fig. 4A in the position of the mutated amino acids. N227 is on the extracellular side but points more away from a putative extracellular funnel region. Ile233 is pointing more towards the inter-TMVI-XI space, still in association with Leu465. Amino acid Leu243 is in a similar position as in Fig. 4A. The acidic amino acids Glu247 and Glu248 face in near opposite directions to each other. Glu247 is in a similar position as in Fig. 4A, while the relative position of Glu248 has changed markedly, now on the intracellular loop rather than part of the TM helix, and it points more towards the space between the TM segments. Both residues are on the cytosolic side of the membrane.

4. Discussion

4.1. TMVI in NHE1 function

The mechanism of Na$^+$/H$^+$ exchange is a question of significant interest both as a basic biological problem, and because of the critical role that the NHE1 protein plays in both heart disease, cell growth and differentiation, and in metastasis of tumor cells. In the E. coli Na$^+$/H$^+$ exchanger, NhaA, TM's IV and XI play a critical role in Na$^+$/H$^+$ exchange. Both these helices are discontinuous, interrupted by an extended segment and the discontinuous helices form mid-membrane dipoles. The ion binding site of NhaA is formed around the extended segments of TMs IV and XI and includes a cluster of amino acids (Asp164, Asp163, Asp133 and Thr132) [29,34]. We recently examined the structure and properties of TMVI of NHE1. We showed that it is a
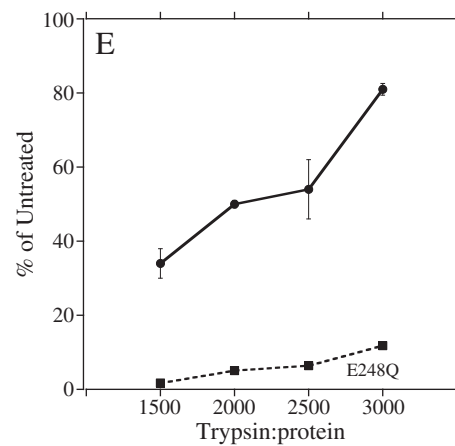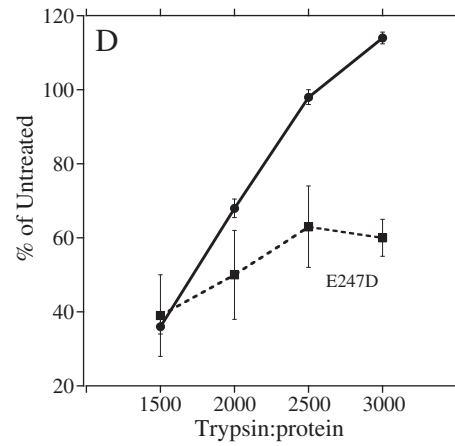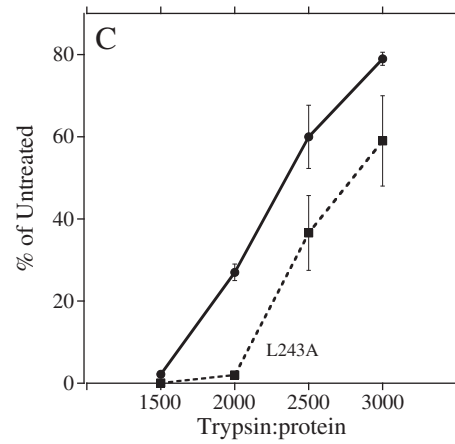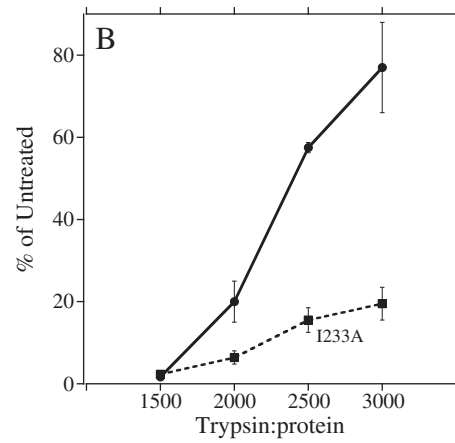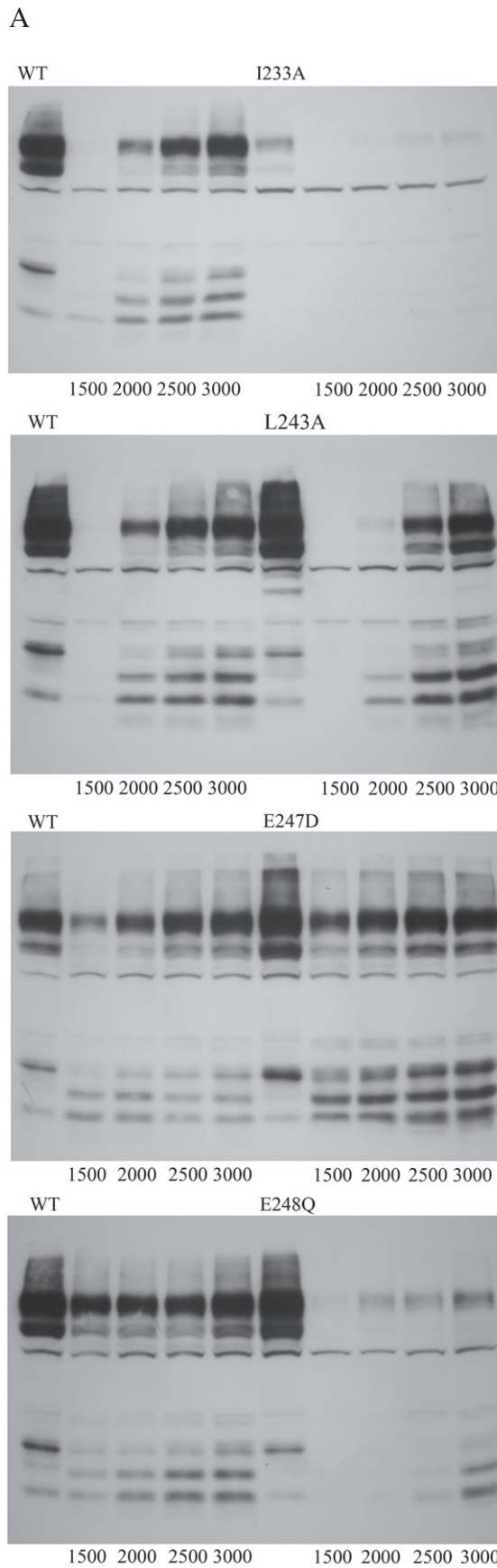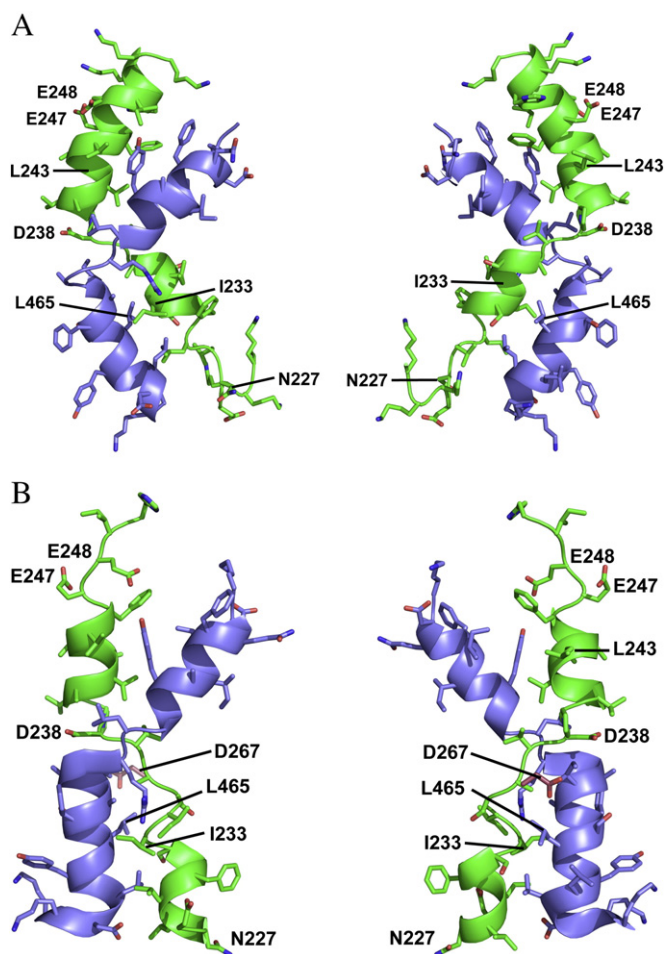
Fig. 4. Model of TMVI/TMXI assembly. A. Model of discontinuous helix assemblies in NHE1 using NMR and artificial restraints. The model was generated using NMR restraints from the structure determination of the individual helices TMVI (residues 226–250) and TMXI (residues K447-K472) combined with distances from the model determined by Landau et al. [22]. Additional terminal lysine tags present in the TMVI peptide structure, but not in the native sequence, are included. TMVI is shown in green, and TMXI is shown in blue. Residues in TM VI which were mutated in this study are labeled. The right diagram is a 180° rotation of the structure. B. Model of discontinuous helices in NHE1 determined by Landau et al. [22]. The diagram shows the predicted structure of TMVI and TMXI as determined by Landau et al. [22] (who describe them as TM4 and TM11 respectively). TMVI (TM4) (residues D226-H250) is shown in green and TMXI (TM11) (residues K447-K472) is shown in blue. Residues in TMVI which were mutated in this study are labeled. The right diagram is a 180° rotation of the structure. The side chain of D267 from TMVII (TM5) (residues 253–273) is shown in red.z

critical TM segment containing the pore lining amino acids Asn227, Ile233 and Leu243 that are accessible from the extracellular aqueous phase. TMVI had an architecture similar to that of TMIV of NhaA, with two helical parts being interrupted by an extended mid membrane segment [27]. TMIV of NHE1 had a smaller amount of similarity to TMIV of NhaA. It had only one helical region consisting of amino acids 169–176 [21]. We also found that another TM fragment of NHE1, TMXI, had the helix-discontinuous region-helix structure, similar to that of TMXI of NhaA. It also possesses pore lining residues [25].

4.2. Functional analysis

In the present study, we further characterized some of the critical amino acids of TMVI. As noted above, amino acids Asn227, Ile233 and Leu243 were earlier shown to be pore lining amino acids, being reactive with MTSET applied from the extracellular surface. In addition, we earlier found that mutation of amino acids Glu247 and Glu248 to Cys resulted in an inactive and partially active protein respectively. The E248C mutant was also partially inhibited with externally applied MTSET [27]. We therefore further characterized these five amino acids in efforts to determine what role they played in NHE1 function. Asn227 was substituted to Ala, Asp, and Arg. Ile233 and Leu243 were mutated to Ala and Glu247 and Glu248 were mutated to Asp and Gln respectively. Asn227 is clearly an important though not essential amino acid. None of the mutations in Asn227 were very well tolerated; N227C [27] and N227R (present study) expressed reduced amounts of NHE1 and only the immature form of NHE1 respectively. N227A and N227D exhibited diminished NHE1 activity and had some mistargeting. Asn contains an uncharged polar side chain, and substitution to alanine had the least effect on NHE1 activity. When Asn227 was mutated into negatively charged Asp, the activity of NHE1 dropped to 40% of control. Substituting positively charged Arg for Asn227 seemed to be the most unfavorable. It resulted in virtual elimination of activity, mistargeting of the protein and decreased expression. The positive charge introduced by Arg could affect sodium coordination, or could destabilize other balancing electrostatic forces within the membrane. This could lead to conformational changes in the protein which led to loss of production of the fully glycosylated protein. Overall, our results with this amino acid suggest that it is pore lining, though not absolutely essential.

Ile233 and Leu243 were also shown earlier to be important pore lining amino acids [27]. For both of these amino acids, mutation to Ala eliminated NHE1 activity. The decrease in activity was not accounted for by decreased protein expression levels or by decreased targeting to the cell surface. These results demonstrate that these amino acids are not only pore lining, but their side chain is critical to the maintenance of NHE1 activity. That mutation to the small uncharged Ala caused so dramatic an effect on activity, further indicates that these amino acids are critical in NHE1 function. Limited digestions with trypsin did suggest a possible change in the conformation of the I233A mutant, though this analysis was not as clear because of the lower expression level of this protein. The L243A mutant protein did show a slight change in accessibility to trypsin, indicating a change in protein conformation. We suggest that mutation of this pore lining amino acid to a smaller one affects the protein folding or stability, which affects its accessibility to trypsin and also affects ion binding and transport. It should be pointed out that our analysis of changes in protein conformation was done using the C-terminal HA tag. Thus it is possible that other changes in the N-terminal region were not detected by our assay and new fragments not containing the HA tag would not be detected.

Analysis of amino acids Glu247 and Glu248 was quite revealing. We earlier demonstrated that mutation of these residues to Cys compromised NHE1 activity and that Glu248 was at least partially pore lining [27]. These results were intriguing and partially led to the decision to further investigate these amino acids. Also, we have earlier [35] suggested that the negative charge that these side chains impart, could aid in cation coordination. Therefore, we investigated the effect of neutralizing and modifying the charge in these positions. We obtained different results with these two amino acids. Neutralizing the charge on Glu247 had no effect on NHE1 activity, while changing

Fig. 3. Limited trypsin digestion of selected TMVI mutants. A. Western blots of WT NHE1, E247D, E248Q, L243A, and I233A whole cell lysates treated with trypsin:protein ratios of 0:1, 1:1500, 1:2000, 1:2500, and 1:3000 as indicated. The pattern of NHE1 digestion was detected using anti-HA antibodies. Similar results were reproduced at least two times. B–E. Summary of results of digestion of WT and mutant NHE1. The relative levels of fully glycosylated NHE1 were compared for WT and mutant NHE1 proteins. The levels of each mutant are compared with that of the WT done simultaneously and run on the same gel.

to the smaller Asp residue noticeably inhibited activity. In contrast, changing Glu248 to Asp, had no effect on NHE1 activity while changing to Gln, caused a precipitous decline in NHE1 activity that was accompanied by a change in conformation of the protein. These results demonstrate that the charge on Glu247 is unimportant in activity, while the location and size of the amino acid is more critical. At position 248, the charge is critical and a small change in the position of the carboxyl group was not of great significance. We suggest that at amino acid 248, the carboxyl is involved in cation coordination and/or maintenance of the coordination structure or sphere of the NHE1 protein. A mutation at this amino acid, neutralizing the carboxyl group, destabilized the conformation of the protein.

4.3. Structure and function of the critical fold of NHE1

As noted above, TMVI of NHE1 resembles TMIV of NhaA, more so than does TMIV. It also has more pore lining amino acids, as determined by cysteine scanning mutagenesis [27]. In addition, we earlier noted that TMXI of NHE1 is similar to TMXI of NhaA [25]. We therefore suggest that TMVI and TMXI constitute the critical catalytic fold of NHE1, similar to TMIV and TMXI of NhaA. Landau et al. [22] have also suggested that TMVI and TMXI play the equivalent role to TMIV and XI of NhaA. Their model suggests that the amino acids of "TMVI" are actually TMIV, (the first two TM segments of NHE1 being removed as a signal sequence) and thus they propose a critical TMIV–TMXI structure. Recently Nygaard et al. [36] modeled the NHE1 protein. Their modeling suggests that TMIV (amino acids 160–179) and TMXI are the critical fold in NHE1 and are similar to TMIV and TMXI of NhaA. Their modeling also suggested that Asp172 of TMIV and Arg425 of TMX have dipole masking functions. However, we have shown that the charge on Asp172 is unnecessary for NHE1 function [37]. Mutation of this residue to Gln did not affect NHE1 activity and mutation to Asn only slightly reduced activity [37]. Thus, the charge at this amino acid is not necessary to NHE1 function and it is unlikely to have a dipole masking function. In addition, as noted above, TMVI of NHE1 is much more similar to TMIV of NhaA, than is TMIV of NHE1. Thus we suggest that TMVI and TMXI are much more likely candidates for the critical fold mediating NHE1 transport.

We therefore examined the putative structure of the TMVI and TMXI region and the location of the critical amino acids of TMVI. The entire structure of the NHE1 protein is unavailable; however, we have earlier [25,27] determined the structure of peptides representing TMVI and TMXI, and Landau et al. [22] have modeled this region based on comparison with NhaA. Fig. 4, depicts two models of the TMVI/XI assembly [22,25], one based on the NMR derived structures of the TM segments (Fig. 4A) and one from the model of Landau et al. [22] (Fig. 4B). The positions of Asn227, Ile233, Leu243, Glu247 and Glu248 are indicated as well as some other critical nearby amino acids. In general the overall architecture of the model based on the determined NMR structures and the model base on that of Landau et al. [22] are similar but there are differences in the position of the side chains as noted below. Both Fig. 4A and B illustrate that Asp238 lies between the assembly of discontinuous helices TMVI/XI, and it may compensate for the positive polarity contributed by the N-terminal ends. Previously we demonstrated that substituting Asp238 with Cys resulted in a dysfunctional NHE1 protein [27]. When considered in the context of the whole model [22] Fig. 4B shows that the side chain of Leu243 is pointing towards the same face of the membrane as a putative protonation site at Asp267. This position is similar in the empirically based NMR model (Fig. 4A). Asp267 is also located in close proximity to the pore lining residues Ile233 and Leu465, which might explain their sensitivity to mutation [22,25,27]. Given that Leu465, Ile233 were pore lining, and that Asp267 is the putative protonation site, it appears as though this region defines at least part of the

channel and transport site of the protein. Clearly mutation or derivation of amino acids in this region is detrimental to the function of NHE1 as demonstrated by mutation to amino acids Asp267, Ile233 and Leu465 [25–27]. Furthermore, studies in NhaA suggest that movement occurs in this region during activation and transport, which could also explain the pore accessibility we observed [38,39].

While it is uncertain which model is closer to the true structure of NHE1, some features of each model correlate better with the data we obtained. The charge on Glu247 was not essential while that on Glu248 was. In addition we [27] found that when Glu248 was mutated to Cys, reaction with MTSET partially inhibited the protein, suggesting it is at least partially pore lining. In the NMR structure based model Glu248 points more away from a putative coordination sphere and is in a helical region while in the model of Landau et al. [22], Glu248 is part of a flexible loop and appears to point more towards the putative cytoplasmic coordination sphere, which could be important in attraction of H^+'s for transport and is more in accordance with our effects on function. Conversely, Asn227 was intolerant of mutation and clearly an important amino acid. Mutation to a positively charged amino acid was most detrimental, in keeping with a putative role in a coordination sphere of a cation. In Fig. 4B Asn227 points further away from a coordination sphere while in the NMR based model (Fig. 4A), it is part of a flexible region possibly in the extracellular loop, where it could be more oriented towards a putative coordination region, which is in greater accordance with its function. Other amino acids have less variation in their position between the two models. It should be noted that overall, both models were quite similar and differences could represent a limitation in solving the structures of single isolated helices or different conformations of the protein during the reaction cycle.

4.4. Conclusion

In conclusion, the critical amino acids of TMVI, Asn227, Ile233, Leu243, Glu247 and Glu248, contribute significantly to the normal function of NHE1. Asn227 is essential in protein expression, processing and activity. The pore lining Ile233 may locate close to Asp267 and Leu265 and is essential for NHE1 activity, perhaps forming part of a narrowing cation access channel or a trimming region. Leu243 is another pore lining residue that contributes to Na^+/H^+ transport and protein stability/conformation. Glu247 and Glu248 are most likely involved in cation transport or protein stability as well, with Glu248 important in protein stability and conformational folding and the charge on Glu248 being critical in protein function. We suggest that TMVI makes up part of a critical fold of NHE1, similar to that which occurs in NhaA. A full length high resolution structure of NHE1 is desirable to confirm these observations and solve the mechanism of mammalian Na^+/H^+ translocation.

Supplementary materials related to this article can be found online at doi:10.1016/j.bbamem.2011.05.004.

Acknowledgements

References

[1] C. Sardet, A. Franchi, J. Pouysségur, Molecular cloning, primary structure, and expression of the human growth factor-activatable Na^+/H^+ antiporter, Cell 56 (1989) 271–280.
[2] L. Fliegel, Regulation of myocardial Na^+/H^+ exchanger activity, Basic Res. Cardiol. 96 (2001) 301–305.

[3] L. Fliegel, The Na$^+$/H$^+$ exchanger isoform 1, Int. J. Biochem. Cell Biol. 37 (2005) 33–37.

[4] G. Kemp, H. Young, L. Fliegel, Structure and function of the human Na$^+$/H$^+$ exchanger isoform 1, Channels (Austin) 2 (2008) 329–336.

[5] L. Fliegel, Regulation of the Na$^+$/H$^+$ exchanger in the healthy and diseased myocardium, Expert Opin. Ther. Targets 13 (2009) 55–68.

[6] L. Counillon, J. Pouyssegur, The expanding family of eukaryotic Na$^+$/H$^+$ exchangers, J. Biol. Chem. 275 (2000) 1–4.

[7] H. Wang, D. Singh, L. Fliegel, The Na+/H+ antiporter potentiates growth and retinoic-acid induced differentiation of P19 embryonal carcinoma cells, J. Biol. Chem. 272 (1997) 26545–26549.

[8] X. Li, P. Karki, L. Lei, H. Wang, L. Fliegel, Na+/H+ exchanger isoform 1 facilitates cardiomyocyte embryonic stem cell differentiation, Am. J. Physiol. Heart Circ. Physiol. 296 (2009) H159–H170.

[9] X. Li, D. Alvarez, J.W. Casey, L.D. Barber, The changing face of the Na$^+$/H$^+$ exchanger, NHE1: structure, regulation, and cellular actions, Annu. Rev. Pharmacol. Toxicol. 42 (2002) 527–552.

[10] C. Stock, A. Schwab, Role of the Na/H exchanger NHE1 in cell migration, Acta Physiol. (Oxf.) 187 (2006) 149–157.

[11] M. Karmazyn, Role of NHE-1 in cardiac hypertrophy and heart failure, in: M. Karmazyn, M. Avkiran, L. Fliegel (Eds.), The Na$^+$/H$^+$ Exchanger, From Molecular to Its Role in Disease, Kluwer academic Publishers, Boston/Dordrecht/London, 2003, pp. 211–219, 318 pp.

[12] G. Busco, R.A. Cardone, M.R. Greco, A. Bellizzi, M. Colella, E. Antelmi, M.T. Mancini, M.E. Dell'Aquila, V. Casavola, A. Paradiso, S.J. Reshkin, NHE1 promotes invadopodial ECM proteolysis through acidification of the peri-invadopodial space, FASEB J. 24 (2010) 3903–3915.

[13] L. Fliegel, Molecular biology of the myocardial Na+/H+ exchanger, J. Mol. Cell. Cardiol. 44 (2008) 228–237.

[14] R.A. Cardone, V. Casavola, S.J. Reshkin, The role of disturbed pH dynamics and the Na$^+$/H$^+$ exchanger in metastasis, Nat. Rev. Cancer 5 (2005) 786–795.

[15] M. Avkiran, A.R. Cook, F. Cuello, Targeting Na$^+$/H$^+$ exchanger regulation for cardiac protection: a RSKy approach? Curr. Opin. Pharmacol. 8 (2008) 133–140.

[16] P. Theroux, B.R. Chaitman, N. Danchin, L. Erhardt, T. Meinertz, J.S. Schroeder, G. Tognoni, H.D. White, J.T. Willerson, A. Jessel, Inhibition of the sodium–hydrogen exchanger with cariporide to prevent myocardial infarction in high-risk ischemic situations. Main results of the GUARDIAN trial. Guard during ischemia against necrosis (GUARDIAN) Investigators, Circulation 102 (2000) 3032–3038.

[17] H.J. Rupprecht, J. vom Dahl, W. Terres, K.M. Seyfarth, G. Richardt, H.P. Schultheibeta, M. Buerke, F.H. Sheehan, H. Drexler, Cardioprotective effects of the Na(+)/H(+) exchange inhibitor cariporide in patients with acute anterior myocardial infarction undergoing direct PTCA, Circulation 101 (2000) 2902–2908.

[18] S. Harguindey, J.L. Arranz, M.L. Wahl, G. Orive, S.J. Reshkin, Proton transport inhibitors as potentially selective anticancer drugs, Anticancer Res. 29 (2009) 2127–2136.

[19] L. Counillon, J. Pouyssegur, R.A. Reithmeier, The Na$^+$/H$^+$ exchanger NHE-1 possesses N- and O-linked glycosylation restricted to the first N-terminal extracellular domain, Biochemistry 33 (1994) 10463–10469.

[20] M.E. Malo, L. Fliegel, Physiological role and regulation of the Na$^+$/H$^+$ exchanger, Can. J. Physiol. Pharmacol. 84 (2006) 1081–1095.

[21] E.R. Slepkov, J.K. Rainey, X. Li, Y. Liu, F.J. Cheng, D.A. Lindhout, B.D. Sykes, L. Fliegel, Structural and functional characterization of transmembrane segment IV of the NHE1 isoform of the Na$^+$/H$^+$ exchanger, J. Biol. Chem. 280 (2005) 17863–17872.

[22] M. Landau, K. Herz, E. Padan, N. Ben-Tal, Model structure of the Na$^+$/H$^+$ exchanger 1 (NHE1): functional and clinical implications, J. Biol. Chem. 282 (2007) 37854–37863.

[23] E.R. Slepkov, S. Chow, M.J. Lemieux, L. Fliegel, Proline residues in transmembrane segment IV are critical for activity, expression and targeting of the Na$^+$/H$^+$ exchanger isoform 1, Biochem. J. 379 (2004) 31–38.

[24] K. Moncoq, G. Kemp, X. Li, L. Fliegel, H.S. Young, Dimeric structure of human Na+/H+ exchanger isoform 1 overproduced in Saccharomyces cerevisiae, J. Biol. Chem. 283 (2008) 4145–4154.

[25] B.L. Lee, X. Li, Y. Liu, B.D. Sykes, L. Fliegel, Structural and functional analysis of transmembrane XI of the NHE1 isoform of the Na$^+$/H$^+$ exchanger, J. Biol. Chem. 284 (2009) 11546–11556.

[26] J. Ding, J.K. Rainey, C. Xu, B.D. Sykes, L. Fliegel, Structural and functional characterization of transmembrane segment VII of the Na$^+$/H$^+$ exchanger isoform 1, J. Biol. Chem. 281 (2006) 29817–29829.

[27] J. Tzeng, B.L. Lee, B.D. Sykes, L. Fliegel, Structural and functional analysis of transmembrane segment VI of the NHE1 isoform of the Na+/H+ exchanger, J. Biol. Chem. 285 (2010) 36656–36665.

[28] R. Murtazina, B.J. Booth, B.L. Bullis, D.N. Singh, L. Fliegel, Functional analysis of polar amino-acid residues in membrane associated regions of the NHE1 isoform of the mammalian Na$^+$/H$^+$ exchanger, Eur. J. Biochem. 268 (2001) 4674–4685.

[29] C. Hunte, E. Screpanti, M. Venturi, A. Rimon, E. Padan, H. Michel, Structure of a Na$^+$/H$^+$ antiporter and insights into mechanism of action and regulation by pH, Nature 435 (2005) 1197–1202.

[30] C.D. Schwieters, J.J. Kuszewski, N. Tjandra, G.M. Clore, The Xplor-NIH NMR molecular structure determination package, J. Magn. Reson. 160 (2003) 65–73.

[31] S. Wakabayashi, T. Pang, X. Su, M. Shigekawa, Second mutations rescue point mutant of the Na(+)/H(+) exchanger NHE1 showing defective surface expression, FEBS Lett. 487 (2000) 257–261.

[32] T. Hisamitsu, Y. Ben Ammar, T.Y. Nakamura, S. Wakabayashi, Dimerization is crucial for the function of the Na+/H+ exchanger NHE1, Biochemistry 45 (2006) 13346–13355.

[33] M. Ndayizeye, N. Touret, L. Fliegel, Proline 146 is critical to the structure, function and targeting of sod2, the Na$^+$/H$^+$ exchanger of Schizosaccharomyces pombe, Biochim. Biophys. Acta. 1788 (2009) 983–992.

[34] E. Padan, The enlightening encounter between structure and function in the NhaA Na+—H+ antiporter, Trends Biochem. Sci. 33 (2008) 435–443.

[35] P. Dibrov, L. Fliegel, Comparative molecular analysis of Na$^+$/H$^+$ exchangers: a unified model for Na$^+$/H$^+$ antiport? FEBS Lett. 424 (1998) 1–5.

[36] E.B. Nygaard, J.O. Lagerstedt, G. Bjerre, B. Shi, M. Budamagunta, K.A. Poulsen, S. Meinild, R.R. Rigor, J.C. Voss, P.M. Cala, S.F. Pedersen, Structural modeling and electron paramagnetic resonance spectroscopy of the human Na+/H+ exchanger isoform 1, NHE1, J. Biol. Chem. 286 (2010) 634–648.

[37] E. Slepkov, J. Ding, J. Han, L. Fliegel, Mutational analysis of potential pore-lining amino acids in TM IV of the Na(+)/H(+) exchanger, Biochim. Biophys. Acta 1768 (2007) 2882–2889.

[38] E. Olkhova, E. Padan, H. Michel, The influence of protonation states on the dynamics of the NhaA antiporter from Escherichia coli, Biophys. J. 92 (2007) 3784–3791.

[39] M. Appel, D. Hizlan, K.R. Vinothkumar, C. Ziegler, W. Kuhlbrandt, Conformations of NhaA, the Na+/H+ exchanger from Escherichia coli, in the pH-activated and ion-translocating states, J. Mol. Biol. 388 (2009) 659–672.